Direct current circuit simulation model for a field emission triode

Chih-Wen Lu and Chung Len Lee

Citation: Journal of Vacuum Science & Technology B **16**, 2876 (1998); doi: 10.1116/1.590241
View online: http://dx.doi.org/10.1116/1.590241
View Table of Contents: http://scitation.aip.org/content/avs/journal/jvstb/16/5?ver=pdfcov
Published by the AVS: Science & Technology of Materials, Interfaces, and Processing

Direct current circuit simulation model for a field emission triode

Chih-Wen Lu and Chung Len Lee[a)]
Department of Electronics Engineering, National Chiao Tung University, Hsinchu, Taiwan, Republic of China

(Received 12 January 1998; accepted 26 June 1998)

A simple empirical circuit model, which can be incorporated into circuit simulation programs such as SPICE, for a field emission triode is developed. The model is based on the Fowler-Nordheim (FN) *J-E* relationship but takes into account the space charge effect and the exponential-like charge distribution on the surface of the tip of the device. A procedure is also developed to extract the parameters of the model. © *1998 American Vacuum Society.* [S0734-211X(98)02105-2]

I. INTRODUCTION

A field emission triode (FET) is a solid-state device which features a miniature vacuum tube triode formed by the application of modern integrated circuit (IC) processing technology. A typical FET consists of a cathode, a control gate and an anode similar to that of a conventional vacuum tube triode, as shown in Fig. 1. When a moderate voltage is applied between the gate and the cathode, a very large electric field is formed on the tip of the cathode due to the sharp geometry of the tip and the short gate-to-cathode distance. An electron will be emitted from the surface of the cathode following the Fowler-Nordheim tunneling mechanism to the anode which is biased at a proper high voltage.[1–3] However, since the gate is always biased more positively than the cathode, large gate currents can flow at zero and moderate positive anode voltage. The cathode current characteristics, the gate current characteristics, and the output characteristics are shown in Figs. 2(a)–2(c), respectively.[4] As the anode voltage decreases, the anode current decreases and the gate current increases. The cathode current is always equal to the anode current plus the gate current.

Applications of FET circuits have triggered a demand for circuit simulation, which requires an efficient and accurate FET model. Some work was done on FET modeling.[5–7] For example, based on the ideal field emitter floating sphere model, Nicolaescu and Avramescu[5] developed a field emission diode model. Jones *et al.*[6] developed a circuit model for a FET array operating at low voltage and characterized the model parameters by using theoretical and experimental techniques. Qin *et al.*[7] also developed a model for the FET amplifier. However, all these models are either fairly complicated or physical structure dependent and none of the models includes the space charge effect which makes the *J-E* relationship of the device deviate from the Fowler-Nordheim (FN) *J-E* relationship in the high gate voltage region.[8,9]

In this work, we propose a FET model which is based on the FN *J-E* relationship but takes into account the space charge effect and the exponential-like charge distribution on the surface of the tip of the device.[9] The model is simple, accurate and easy to incorporate into a circuit simulation program such as SPICE.

a)Electronic mail: cllee@cc.nctu.edu.tw

II. DEVICE MODEL

The proposed device equivalent circuit is shown in Fig. 3. The anode and gate currents are both functions of anode voltage V_a and gate voltage V_g. The anode current can be obtained by subtracting the gate current from the cathode current.

The cathode current I_c, mainly based on the Fowler-Nordheim relationship, is expressed as

$$I_c(V_g)=A_c V_g^2 \exp\left[-\frac{B_c}{V_g}-C\exp\left(\frac{D}{V_g}\right)\right], \tag{1}$$

where A_c is a parameter related to the field enhanced parameter **a** and the effective emission area **b** by $\sim$**b**/**a**2, B_c is E_c**a**, where E_c is the critical electrical field,[10–14] and C and D are two parameters related to the space charge effect. When the device is operated at low gate bias, C and D are zero and Eq. (1) can be simplified to

$$I_c(V_g)=A_c V_g^2 \exp\left[-\frac{B_c}{V_g}\right], \tag{2}$$

which is the typical FN equation.[2,3,10,15] In the above equations, the cathode voltage is assumed to be the reference grounded voltage.

Figure 4 shows the FN plot of the cathode current of the experimental device of Figs. 2(a)–2(c).[4] In the plot, it can be seen that the plot is a straight line at the low gate voltage region and bends at the high gate voltage region due to the

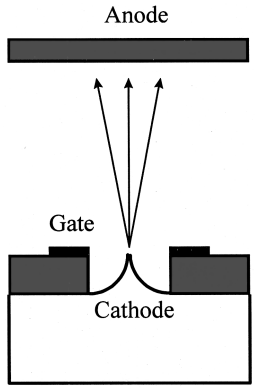

FIG. 1. Typical field emission transistor consisting of a cathode, a control gate and an anode.

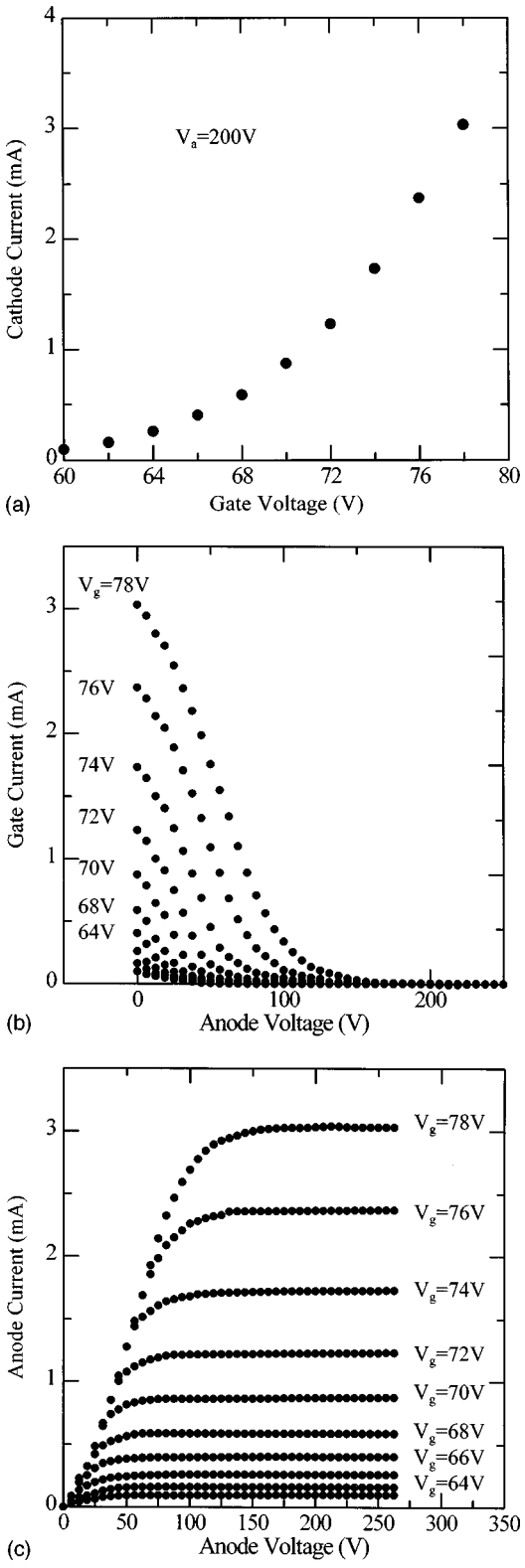

FIG. 2. (a) Characteristics of the cathode current of a FET measured with gate voltages varying from 60 to 78 V. (b) Characteristics of the gate current of the same device for which, as the anode voltage increases, the gate current decreases. (c) Output characteristics of the same device for which, as the anode voltage increases, the anode current increases.

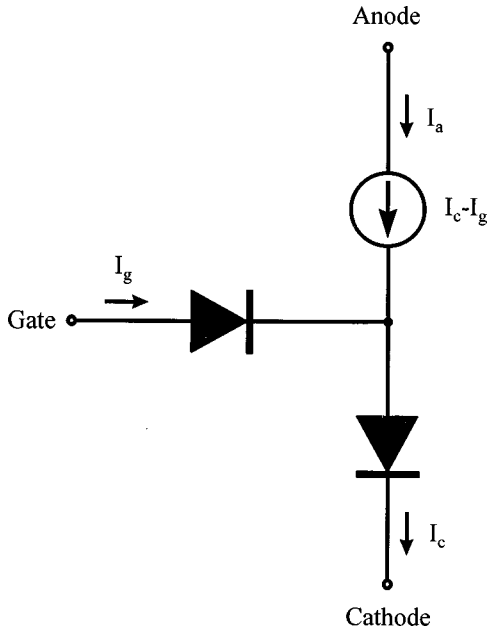

FIG. 3. Proposed device equivalent circuit. The cathode and gate currents are both functions of anode voltage V_a and gate voltage V_g. The anode current can be obtained by subtracting the gate current from the cathode current.

space charge effect. From this plot, parameters A_c, B_c, C and D can be determined, which will be explained in Sec. III.

The cathode current is shared by the anode and the gate. It is known that the gate current equals the cathode current when the anode voltage is zero. That is,

$$I_g(V_a=0)=I_c. \tag{3}$$

The above equation can be considered to be the boundary condition for deriving the gate current expression.

At the above boundary condition, the gate current expression should be the same as that of the cathode current, i.e.,

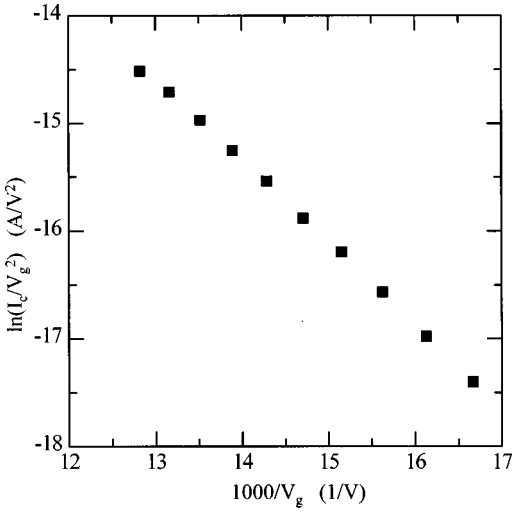

FIG. 4. FN plot of the cathode current of an experimental device operating at $V_a=200$ V. The plot is a straight line at the low gate voltage region and bends at the high gate voltage region due to the space charge effect.

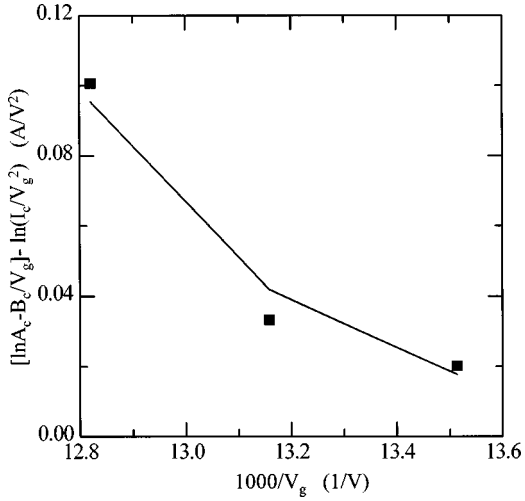

FIG. 5. Plot of the difference between $\ln A_c - (B_c/V_g)$ and $\ln(I_c/V_g^2)$ with respect to $1000/V_g$ from which the values of C and D can be extracted.

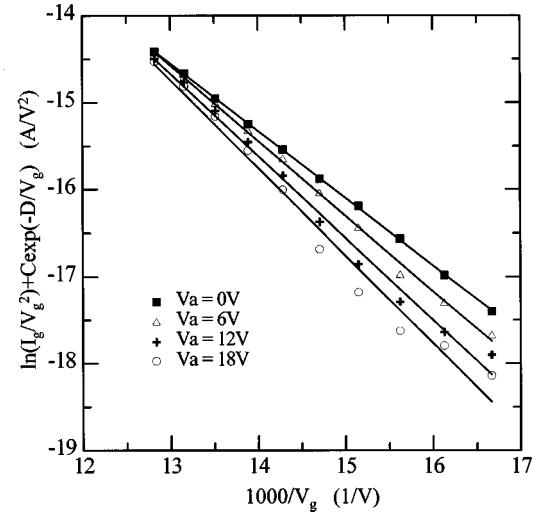

FIG. 6. FN plot of the gate current of the experimental device for several V_a's from which the values of the anode-voltage-dependent factors, $\ln A_c + E_1 V_a + E_2 V_a^2$ and $B_c + F_1 V_a + F_2 V_a^2$, are calculated from the slope and the intercept of the coordinate axis for each anode voltage.

$$I_g(V_a=0,V_g)=A_g(V_a=0)V_g^2 \exp\left[-\frac{B_c}{V_g}-C \times \exp\left(-\frac{D}{V_g}\right)\right], \tag{4}$$

where $A_g(V_a=0)=A_c$ and it is also related to the field enhanced parameter and the effective emission area. The field enhanced parameter should be the same as that in the cathode current expression. The effective emission area is dependent on the anode and gate voltages. A larger gate voltage and a smaller anode voltage give a larger gate current. So, A_g is a function of V_g and V_a. The current density distribution of the surface of the tip is an exponential-like decay.[9] We express A_g in the following form:

$$A_g=A_c \exp\left(E_1 V_a+E_2 V_a^2-\frac{F_1 V_a+F_2 V_a^2}{V_g}\right), \tag{5}$$

where E_1, E_2, F_1 and F_2 are parameters to be used to fit the effective emission area of the gate current. When the anode voltage is not zero, the gate current can be expressed as

$$I_g(V_a,V_g)=A_c V_g^2 \exp\left[E_1 V_a+E_2 V_a^2 \frac{B_c+F_1 V_a+F_2 V_a^2}{V_g} - C \exp\left(-\frac{D}{V_g}\right)\right]. \tag{6}$$

The anode current can be obtained by subtracting the gate current I_g from the cathode current I_c, i.e.,

$$I_a=I_c-I_g. \tag{7}$$

III. PARAMETER EXTRACTION

As mentioned previously, the parameters can be extracted in values from the measured cathode current and gate current in the FN plots of an experimental device. To describe the procedure more clearly, device data which were published in the literature are used as examples for the demonstration.

The first device example used is that published in Betsui's paper.[4] The device was a silicon field emitter array of 6400 (80×80) tips. The radius of the bullet-shaped tip was less than 20 nm. The spacing between tips was 4 μm, so the tip density was 6.25×10^6 cm^{-2}. The diameter of the gate aperture was 2 μm, which was larger than that of its silicon dioxide mask. The distance between the anode plate and gate was 1 mm. In Betsui's measuring apparatus, the gate was grounded and negative voltage was applied to the cathode to extract electrons. In this work, the cathode voltage is assumed to be the reference grounded voltage. The cathode, the gate, and the output I-V characteristics are those shown in Figs. 2(a)–2(c), respectively.

In Eqs. (1) and (6), A_c, B_c, C, D, E_1, E_2, F_1 and F_2 are unknown parameters. From the FN plot of Fig. 4, the values of A_c and B_c can be obtained from the slope and the intercept of the coordinate axis in the nonspace charge region.[16] The values of A_c and B_c are 1.21×10^{-2} A/V^2 and 7.81×10^2 V, respectively.

The values of parameters C and D can be extracted by rearranging Eq. (1) as

TABLE I. Extracted values for the device model parameters of the experimental device of Ref. 4.

Parameter	Value
A_c	1.21×10^{-2} A/V^2
B_c	7.81×10^2 V
C	3.56×10^{12}
D	44×10^3 V
E_1	2.92×10^{-1} V^{-1}
E_2	2.87×10^{-4} V^{-2}
F_1	2.27×10^1
F_2	3.93×10^{-2} V^{-1}

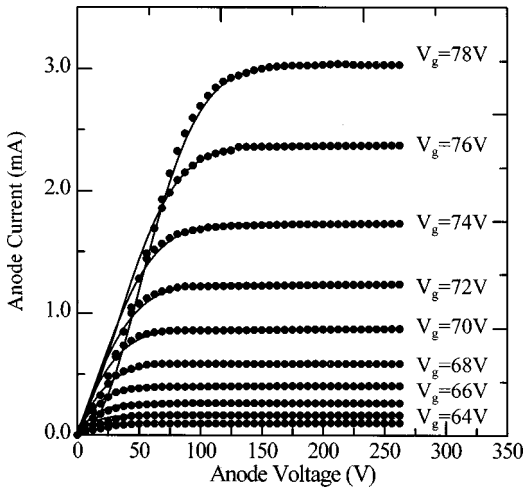

FIG. 7. Reconstructed output characteristics (solid curves) simulated from the extracted values of the circuit parameters and the original measured output characteristics (dotted curves). Two sets of characteristics match very well.

$$\ln A_c - \frac{B_c}{V_g} - \ln \frac{I_c}{V_g^2} = C \exp\left(-\frac{D}{V_g}\right). \tag{8}$$

Since I_c is measured data and the A_c and B_c values are already known, the difference between $\ln A_c - (B_c/V_g)$ and $\ln(I_c/V_g^2)$ can be plotted as shown in Fig. 5, which is an exponential decay curve against $1000/V_g$. The values of C and D can be easily extracted from this plot.

The values of the gate current parameters, E_1, E_2, F_1 and F_2, can be obtained by a similar procedure. Taking the natural logarithm and rearranging the gate current expression of Eq. (6), we obtain

TABLE II. Extracted values for the device model parameters of the experimental device of Ref. 9.

Parameter	Value
A_c	1.01×10^{-2} A/V^2
B_c	5.20×10^{2} V
C	1.11×10^{1}
D	5.88×10^{2} V

$$\ln \frac{I_g}{V_g^2} + C \exp\left(-\frac{D}{V_g}\right) = \ln A_c + E_1 V_a + E_2 V_a^2 - \frac{B_c + F_1 V_a + F_2 V_a^2}{V_g}, \tag{9}$$

where I_g is measured data. The values of E_1, E_2, F_1, and F_2 can be obtained by plotting $\ln(I_g/V_g^2) + C \exp -(D/V_g)$ against $1/V_g$ for each anode voltage V_a in Eq. (9). Figure 6 is the FN plot for an experimental device for several V_a's. The values of the anode-voltage-dependent factors, $\ln A_c + E_1 V_a + E_2 V_a^2$ and $B_c + F_1 V_a + F_2 V_a^2$, can be calculated from the slope and the intercept of the coordinate axis for each anode voltage. Then, the values of E_1, E_2, F_1, and F_2 can be extracted. The values derived for all the parameters are summarized in Table I.

The experimental device above was used to extract the values of the parameters in Eqs. (1), (6) and (7). The values obtained can be used to reconstruct the characteristics of the device. Figure 7 shows the reconstructed output characteristics (the solid curves) of the device along with the originally measured output characteristics (the dotted curves). Two sets of characteristics match very well.

To verify the validity of this model for a field emission cathode operated in the space charge region, a second example is also given. Figure 8 shows the *I-V* characteristics of a Spindt-type FET with a single emitter,[9] where the open circle curve are the data points obtained from Ref. 9 and the

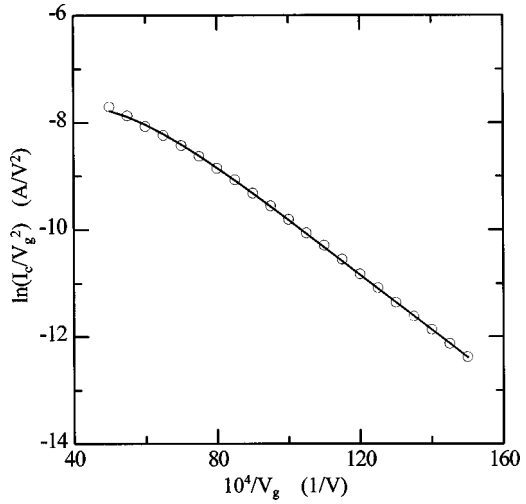

FIG. 8. *I-V* characteristics of a Spindt-type FET with a single emitter (Ref. 9). The open circle curve is the data points obtained from Ref. 9 and the solid line is the reconstructed curve from Eq. (1).

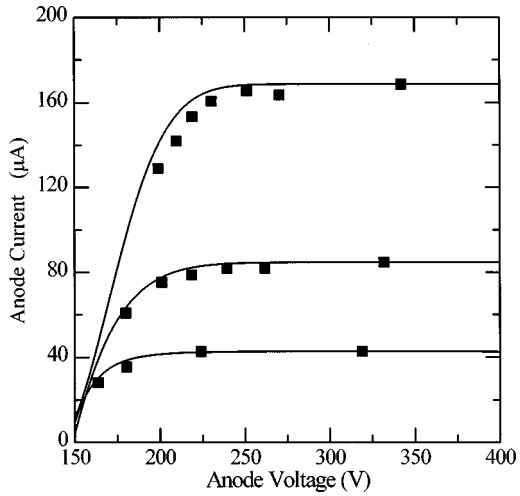

FIG. 9. *I-V* characteristics of a FET triode with 100 emitter tips. The square curves are the data points obtained from Ref. 17 and the solid lines are reconstructed curves from the model.

TABLE III. Extracted values for the device model parameters of the experimental device of Ref. 17.

Parameter	Value
A_c	3.44×10^{-5} A/V^2
B_c	1.79×10^{3} V
E_1	5.31×10^{-1} V^{-1}
E_2	-5.97×10^{-3} V^{-2}
F_1	1.07×10^{2}
F_2	-1.09 V^{-1}

solid line is the reconstructed curve from Eq. (1). At the high field region where the space charge effect becomes evident, the *I-V* deviates from the Fowler-Nordheim straight line characteristics. The two curves show a good match. The values derived for the parameters are summarized in Table II.

A third example of a FET of a different emitter geometry is also used to verify the model. Figure 9 shows the *I-V* characteristics of a FET triode with 100 emitter tips and a separate anode in the form of a tube located 5 mm from the gate electrode,[17] where the square curves are the data points obtained from Ref. 17 and the solid lines are reconstructed curves from the model. This device operates only in the nonspace charge region. So the values of parameters *C* and *D* are zero. Two sets of curves also agree with each other well. The values derived for the parameters are summarized in Table III. This example also demonstrates that the model is applicable to a FET with emitters of tube geometry.

IV. CONCLUSION

In this work, a simple empirical model for a FET device has been developed. The model can be used in circuit simulation programs such as SPICE. For the model, the cathode current is based on the FN relationship but takes into account the space charge effect, and the gate current, which is also based on the FN relationship through the boundary condition, $I_g(V_a=0)=I_c$, considers the exponential-like decay of the charge distribution on the surface of the tip of the device. A procedure to extract the values for the model parameters has also been demonstrated. To obtain the model parameters, six sets of measurements for different gate voltages, three sets for the nonspace charge region and three sets for the space charge region are needed. The model has been applied to experimental FET devices of different geometries, namely, an emitter array, a single emitter and a tube type of anode, to show its applicability. From the successful application to the three device examples of different geometries, it can be said that this model can be applied to describe the Spindt-type FETs.

[1]R. H. Fowler and L. Nordheim, Proc. R. Soc. London **119**, 173 (1928).
[2]C. A. Spindt, I. Brodie, L. Humphrey, and E. R. Westerberg, J. Appl. Phys. **47**, 5248 (1976).
[3]W. J. Orvis, C. F. McConaghy, D. R. Ciarlo, J. H. Yee, and E. W. Hee, IEEE Trans. Electron Devices **36**, 2651 (1989).
[4]K. Betsui, Technical Digest of IVMC'91, 1991, pp. 26–29.
[5]D. Nicolaescu and V. Avramescu, J. Vac. Sci. Technol. B **12**, 749 (1994).
[6]R. D. Jones, R. K. Feeney, J. K. Cochran, and D. N. Hill, Technical Digest of IVMC'95, 1995, pp. 72–76.
[7]M. Qin, Q. A. Huang, and T. L. Wei, Technical Digest of IVMC'96, 1996, pp. 86–90.
[8]R. True, Tech. Dig. Int. Electron Devices Meet., 1992, p. 379.
[9]G. N. A. Van Veen, J. Vac. Sci. Technol. B **12**, 655 (1994).
[10]E. A. Adler, Z. Bardai, R. Forman, D. M. Goebel, R. T. Longo, and M. Sokolich, IEEE Trans. Electron Devices **38**, 2304 (1991).
[11]H. H. Busta, D. W. Jenkins, B. J. Zimmerman, and J. E. Pogemiller, Tech. Dig. Int. Electron Devices Meet., 1991, p. 213.
[12]H. H. Busta, D. W. Jenkins, B. J. Zimmerman, and J. E. Pogemiller, IEEE Trans. Electron Devices **39**, 2616 (1992).
[13]H. H. Busta, J. E. Pogemiller, and B. J. Zimmerman, IEEE Trans. Electron Devices **40**, 1530 (1993).
[14]D. Nicolaescu, Technical Digest of IVMC'94, 1994, pp. 139–142.
[15]D. A. Kirkpatrick, A. Mankofsky, and K. T. Tsang, Appl. Phys. Lett. **60**, 2065 (1992).
[16]J. M. Houston, Phys. Rev. **88**, 349 (1952).
[17]C. E. Holland, A. Rosengreen, and C. A. Spindt, IEEE Trans. Electron Devices **38**, 2368 (1991).